Desalination and Water Treatment
www.deswater.com
doi: 10.1080/19443994.2015.1090914

57 (2016) 18551–18559
August

Taylor & Francis
Taylor & Francis Group

Adsorption kinetics, isotherms, and thermodynamic studies for Hg^{2+} adsorption from aqueous medium using alizarin red-S-loaded amberlite IRA-400 resin

Mu. Naushad[a,*], S. Vasudevan[b], G. Sharma[c], A. Kumar[c], Z.A. ALOthman[a]

[a]*Department of Chemistry, College of Science, Bld#5, King Saud University, Riyadh, Saudi Arabia, Tel. +966 14674198; emails: shad81@rediffmail.com (Mu. Naushad), zaothman@ksu.edu.sa (Z.A. ALOthman)*
[b]*CSIR-Central Electrochemical Research Institute, Karaikudi 630003, India, email: svasudevan65@gmail.com*
[c]*School of Chemistry, Shoolini University, Solan 173212, Himachal Pradesh, India, emails: gaurav8777@gmail.com (G. Sharma), mittuchem83@gmail.com (A. Kumar)*

Received 10 January 2015; Accepted 29 August 2015

ABSTRACT

Alizarin red-S-modified amberlite IRA-400 resin (ARSA) was applied for Hg^{2+} removal from the aqueous medium which is a highly toxic metal ion. The adsorption process which was pH dependent, showed maximum adsorption of Hg^{2+} in the pH range 6–8. ARSA exhibited good monolayer adsorption capacity for Hg^{2+} (303.03 mg g^{-1}) at 25°C and the isotherm was well fitted by the Langmuir model. Moreover, the adsorption was evaluated thermodynamically and the negative values of Gibbs free energy revealed the spontaneity of adsorption process. The practical applicability of ARSA was explored for the adsorption of Hg^{2+} metal ion from a real water sample. The values of ΔH and ΔS were found to be 79.87 kJ mol^{-1} and 0.26 J mol^{-1} K^{-1}, respectively.

Keywords: Amberlite IRA-400; Alizarin red-S; Toxic metals; Hg^{2+}; Adsorption; Kinetics; Real sample

1. Introduction

Adsorption is one of the oldest techniques employed for the removal of contaminants from environment, and still has its immense relevance in the present time [1–5]. With the gradual developments of diverse adsorbent materials, the field of adsorption has become broader and specific in nature for particular pollutants including heavy metals, phenols, antibiotics, and pesticides . [6,7]. The most treacherous of these pollutants are heavy toxic metals, such as lead, chromium, mercury, cadmium, arsenic, and cobalt [8,9]. These toxic metals are non-biodegradable and can risk the human health by being accumulated in the food chain. Among these toxic metal ions, mercury is one of the most toxic, generally found in the environment. The main signs of Hg poisoning are neuronal toxicity, but it also causes serious harm to the kidney, bones, cardiovascular system, etc. [10–12]. The entry of mercury into food chain has been an alarming threat. The mercury ions can be transformed into methylmercury by micro-organisms. Its toxic nature has been known for centuries, but its unique properties lead to the fabrication of various

*Corresponding author.

mercury-based products, such as paints, fungicides, chlor-alkali, pharmaceutical, fluorescent lights, and dental amalgam. [13]. The key sources of Hg^{2+} are coal combustion, base metal smelting, waste incineration, chlor-alkali industry, etc. [14]. Thus, the quantity of mercury unconstrained and mobilized due to human actions has significantly increased, leading to its elevated concentrations in water, air, soil, and living beings. Hence, the removal of mercury in wastewater is very important issue which cannot be ignored. Several techniques are available for the management of mercury waste which includes ion exchange, chemical precipitation, membrane separation, coagulation, solid-phase extraction, biological treatment, and adsorption [15–19]. Among these techniques, adsorption has played an essential role for the remediation and recovery of mercury from wastewater. A large number of adsorbents of high adsorption capacity and selectivity have been synthesized, e.g. activated carbon, nanoparticles, hydrogels, silica-based materials, kaolin–humic acids, biopolymers such as chitin and chitosan, polymeric micro-particles, and ion exchangers. [20–24]. The ion exchange resins have shown exceptional role in metals recovery and separation, and are widely used for pre-concentrating and heavy metal ions removal from wastewater. Furthermore, the efficiency and selectivity for mercury adsorption could be enhanced using some chelating resins coated with polymers or dyes [25]. The mercury ions have a strong affinity towards O, N, and S atoms containing ligands, hence, chelating resins having these ions have been synthesized for the removal of mercury [26–29]. Thus, due to the great concern about mercury pollution in biosphere and its tendency of bioaccumulation in the food chain, the remediation of mercury is a big challenge to the scientists.

The present work provides an insight into the role of alizarin red-S-loaded amberlite IRA-400 anion exchange resin (ARSA) for immobilizing and accumulating mercury, and to minimize the possible toxicity of this metal. The adsorption isotherm models as well as kinetic parameters for the removal of Hg^{2+} were also clarified.

2. Experimental

2.1. Reagents and chemicals

Amberlite IRA-400 (Cl^- form) anion exchange resin and alizarin red-S dye (chemical formula: $C_{14}H_7NaO_7S$) were purchased from Sigma-Aldrich, Germany. The Hg^{2+} stock solution (200 mg mL^{-1}) was prepared and used for further dilutions.

2.2. Preparation of ARSA

For the modification of amberlite IRA-400 resin with the alizarin red-S dye, 0.5 g of amberlite IRA-400 resin was shaken with 50-mL aqueous solution of 500 mg L^{-1} alizarin red-S dye solution at pH 7.0 for 6 h [30]. After the equilibration period, the extra reagent was removed by consecutive washing of the resin with the Milli-Q water, and it was finally dried at 50°C.

2.3. Batch adsorption experiments

The adsorption of Hg^{2+} onto ARSA was performed by batch method. About 50 mg of ARSA was shaken with 50 mL of Hg^{2+} solution of known concentration in the conical flask at room temperature for different time intervals. After attaining the equilibration time, ARSA was filtered off and the concentration of Hg^{2+} in the solution phase was determined by EDTA titration [31–33]. Various parameters viz. pH, contact time, resin dose, initial Hg^{2+} ion concentration, and temperature were also optimized.

The removal efficiency of Hg^{2+} adsorption was calculated as:

$$q_e = \frac{(C_o - C_e)V}{m} \quad (1)$$

Kinetics studies were executed by varying the concentration of Hg^{2+} ion (C_o, 50, 75, and 100 μg L^{-1}). The samples were collected at various time interims until equilibrium was obtained. Isotherm and thermodynamic studies were carried out by changing the reaction temperature (25–50°C) and initial concentration of Hg^{2+} solution (25–125 mg L^{-1}).

Desorption and regeneration studies are very important parameters, which were also carried out by batch process. About 50 mL of 50 mg L^{-1} Hg^{2+} metal ion solution was treated with 50 mg of ARSA in conical flask and shaken for 90 min. After 90 min, ARSA was washed several times with Milli-Q water to remove the excess Hg^{2+}. Then, ARSA was treated with 50 mL of 0.01 M HNO_3 solution in other flask which was again shaken (to desorb Hg^{2+}) for 90 min. The solution was then filtered and the filtrate was treated against the standard solution of 0.01 M di-sodium salts of EDTA to check the desorbed Hg^{2+}. The same procedure was repeated for four successive cycles.

3. Results and discussion

Amberlite IRA-400 resin was modified with alizarin red-S dye and used for Hg^{2+} metal ion removal from aqueous medium. The hydrophobic nature of the

styrene–divinyl benzene matrix of amberlite IRA-400 resin made it an excellent support for the adsorption of alizarin red-S via π–π interaction between the benzene rings of alizarin red-S and amberlite IRA-400 resin. Dipole–dipole interaction also took place between the nitrogen and oxygen atoms of alizarin red-S and amberlite IRA-400 resin, respectively. The modification of amberlite IRA-400 resin using alizarin red-S dye might be given as (Scheme 1).

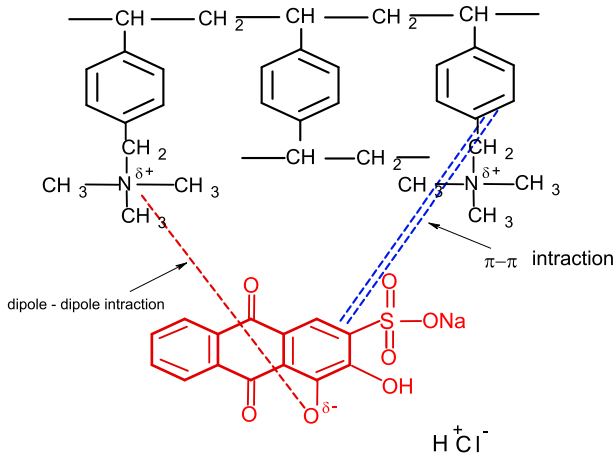

Scheme 1. Interaction of alizarin red-S with amberlite IRA-400 resin.

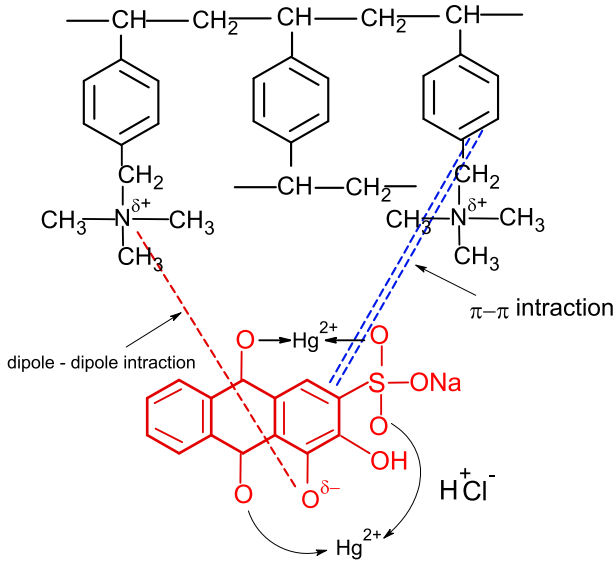

Scheme 2. Bonding of Hg2+ metal ion with alizarin red-S modified amberlite IRA-400 resin.

The alizarin red-S-modified amberlite IRA-400 resin was efficiently applied for Hg^{2+} removal from aqueous medium. Actually, the dye modified resins behave like a chelating resin and chelating resins have revealed enhanced performance to transition metal ions in comparison to the conventional ion exchange

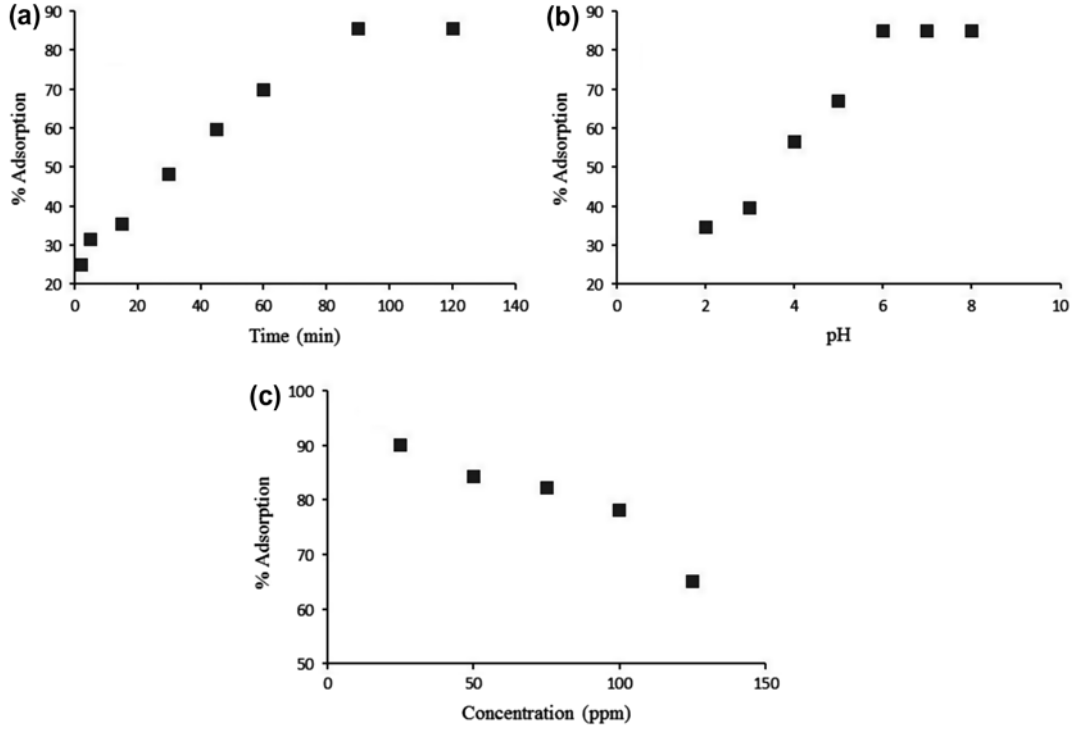

Fig. 1. Percent removal of Hg^{2+} metal ion using ARSA at different (a) time, (b) pH, and (c) initial Hg^{2+} metal ion concentration.

resins [34]. The adsorption of Hg^{2+} metal ion onto ARSA can be shown by the following mechanism (Scheme 2).

The equilibration time for the maximum adsorption of Hg^{2+} was performed at different time interval (2–120 min), and it was noted that the adsorption was rapid at the beginning and equilibrium was established within 90 min, where 85.5% Hg^{2+} metal ion was adsorbed (Fig. 1(a)). The dissimilarity in the adsorption rates was due to the fact that, in the beginning, all sites at the resin surface were vacant, so the adsorption of Hg^{2+}onto ARSA was high. Afterwards, the adsorption became slow due to the decrease in the number of adsorption sites as well as Hg^{2+} concentration [35–37]. The adsorption of Hg^{2+} metal ion onto ARSA was determined in the pH range 2–8, while the other parameters were set constant. It was found that the adsorption of Hg^{2+} was increased from 34.5 to 85% with the increase in pH from 2 to 6 (Fig. 1(b)). After pH 6, there was no change in the adsorption of Hg^{2+} because at pH > 6.0, the Hg^{2+} metal ion gets precipitated. The adsorption of Hg^{2+}onto ARSA was also studied at various concentrations (25–125 mg L^{-1}) of Hg^{2+} metal ion where time and pH were kept 90 min and 6, respectively. The adsorption percentage of Hg^{2+} decreased from 90 to 65% with the increase in the concentration of Hg^{2+} from 25 to 125 mg L^{-1} (Fig. 1(c)). The decrease in the adsorption was due to the less availability of adsorption sites at the surface of ARSA for the higher concentration of Hg^{2+} metal ion. The effect of ARSA dose on the adsorption of Hg^{2+} was also studied (Fig. 2(a)), and it was found that the removal percentage of Hg^{2+} increased from 47.5 to 90.3% with increasing ARSA dose from 0.025 to 0.10 g. This can be clarified as, when the ARSA dose increases, larger surface area will be accessible, which exposed more active sites for the binding of Hg^{2+} metal ions onto ARSA. For the fixed concentration, no change in the percent adsorption of Hg^{2+} was observed after the dosage of 0.10 g. To check the reusability of exhausted ARSA, regeneration studies were conducted for four consecutive cycles (Fig. 3). It was noticed that the adsorption reduced from 86.3 to 76.8%, while desorption reduced from 85 to 71.2%, after four consecutive cycles. This study showed that ARSA was an excellent adsorbent which could be employed for the removal and recovery of Hg^{2+} without any considerable loss in the adsorptive performance.

The practical efficiency of ARSA was explored for the removal of Hg^{2+} metal ion from a water sample which was taken from King Saud University campus, Riyadh, Saudi Arabia. About 50 mg Hg^{2+} was spiked in one liter of this water sample. A known volume (25–75 mL) of this water sample was shaken with 0.10 g of ARSA in the conical flask for 90 min. After 90 min, the solution was filtered, and the filtrate was analyzed. It was noted that more than 83% Hg^{2+} metal ion was adsorbed onto ARSA.

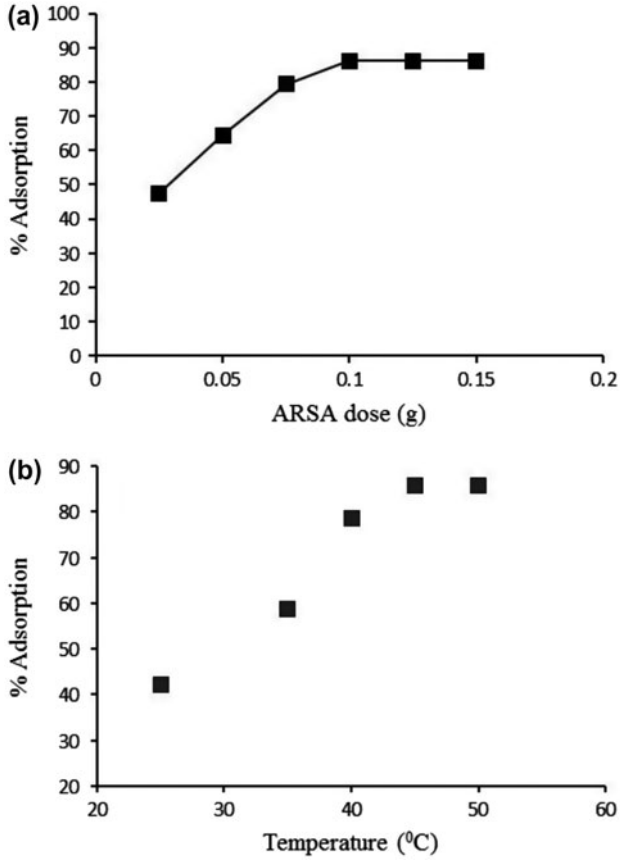

Fig. 2. Percent removal of Hg^{2+} metal ion using ARSA at different (a) ARSA dose and (b) temperature.

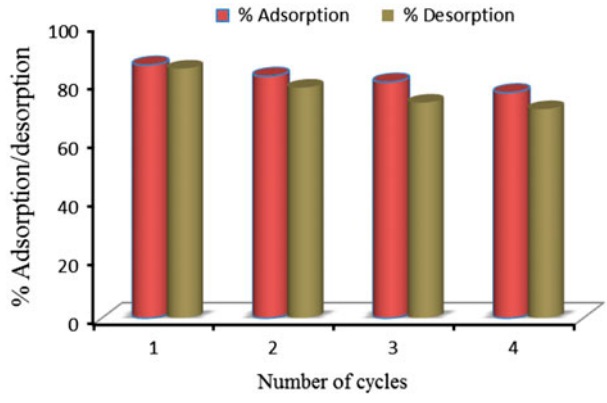

Fig. 3. Adsorption–desorption and regeneration studies of ARSA using 0.01-M HNO_3 solution.

Table 1
Kinetic constant parameters for Hg^{2+} adsorption of onto ARSA

	Pseudo-first-order				Pseudo-second-order			
Initial concentration (mg L^{-1})	Slope	Intercept	k_1 (min^{-1})	R^2	Slope	Intercept	k_2 (10^{-3}) (g mg^{-1} min^{-1})	R^2
50	-9.5×10^{-3}	1.89	2.18×10^{-2}	0.988	0.011	0.096	1.03×10^{-3}	0.960
75	-9.7×10^{-3}	2.01	2.23×10^{-2}	0.989	0.008	0.070	0.91×10^{-3}	0.960
100	-9.9×10^{-3}	2.07	2.28×10^{-2}	0.985	0.006	0.057	0.63×10^{-3}	0.962

3.1. Adsorption kinetics, isotherms, and thermodynamic studies

The effectiveness for the adsorption of Hg^{2+} onto ARSA was evaluated by pseudo-first-order and pseudo-second-order models [38,39]. Different isotherm models [40–42] were applied and numerous thermodynamics parameters were also assessed for the adsorption of Hg^{2+} onto ARSA in the temperature range 298–318 K.

The pseudo-first-order and pseudo-second-order equations are represented as follows:
Pseudo-first-order:

$$\log(q_e - q_t) = \log q_e - \frac{k_1 t}{2.303} \quad (2)$$

Pseudo-second-order:

$$\frac{t}{q_t} = \frac{1}{k_2 q_e^2} + \frac{t}{q_e} \quad (3)$$

The values of rate constants k_1 (min^{-1}) and k_2 (g mg^{-1} min^{-1}) were determined from the slopes of the plots $\log(q_e - q_t)$ vs. t and t/q_t vs. time, respectively. The parameters for these two models are shown in Table 1. It was found that the values of correlation coefficients (R^2) for pseudo-first-order model were higher than pseudo-second-order model, which showed that the studied adsorption system fits to the pseudo-first-order kinetic model (Fig. 4(a) and (b)).

The Langmuir isotherm model can be represented as:

$$\frac{1}{q_e} = \frac{1}{q_m} + \frac{1}{b q_m C_e} \quad (4)$$

A dimensionless equilibrium parameter (R_L) has been defined to evaluate the validity of the Langmuir-type adsorption process:

$$R_L = \frac{1}{1 + bC_o} \quad (5)$$

Freundlich isotherm is expressed by the following equation:

$$\log q_e = \log K_F + \frac{1}{n} \log C_e \quad (6)$$

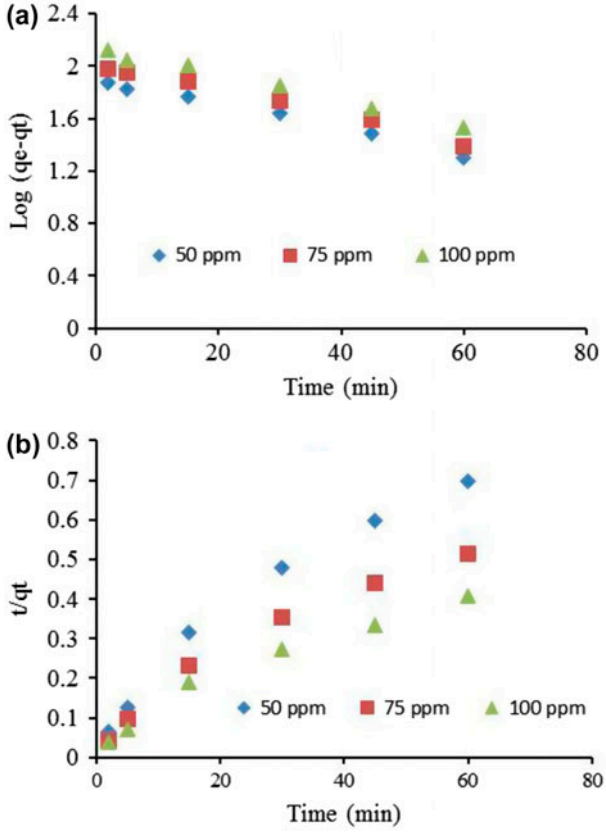

Fig. 4. (a) Pseudo-first-order and (b) pseudo-second-order kinetic models for the adsorption of Hg^{2+} metal ion using ARSA.

Table 2
Adsorption isotherm constants parameters for the adsorption of Hg^{2+} onto ARSA

	Langmuir constants			Freundlich constants				Temkin constants		
Temperature (℃)	Q_m (mg g^{-1})	b (L mg^{-1})	R^2	$1/n$	n	K_F	R^2	B (mg g^{-1})	A	R^2
25	270.27	0.056	0.972	0.59	1.69	24.09	0.982	62.67	1.4	0.956
35	273.97	0.058	0.970	0.59	1.69	24.94	0.982	65.12	1.65	0.953
45	303.03	0.062	0.978	0.56	1.78	28.37	0.988	66.74	1.98	0.955
50	344.8	0.062	0.972	0.53	1.88	31.62	0.986	67.94	2.00	0.955

The linear form of Temkin isotherm model is described as follow:

$$q_e = \frac{RT}{b_T} \ln K_T + \frac{RT}{b_T} \ln C_e \quad (7)$$

where b_T is the Temkin constant related to the heat of sorption (kJ mol^{-1}), K_T is the equilibrium binding constant corresponding to the maximum binding energy (L g^{-1}). In the adsorption isotherm studies, the values of Langmuir constants Q_m and b were assessed from the intercept and slope of linear plots of $1/q_e$ vs. $1/C_e$, respectively. It was found that q_m values were increased with the increase in temperature which showed the endothermic nature for the adsorption of Hg^{2+} onto ARSA (Table 2). The values of dimensionless equilibrium parameter (R_L) was less than unity and greater than zero, which showed the promising adsorption of Hg^{2+} onto ARSA. The values of Freundlich constants K_F and n were evaluated from the slope ($1/n$) and intercept ($\log K_F$) of the plot of $\log q_e$ vs. $\log C_e$, respectively. The parameters obtained by fitting these three isotherm models (Fig. 5(a)–(c)) are given in Table 2. The Freundlich isotherm model showed the

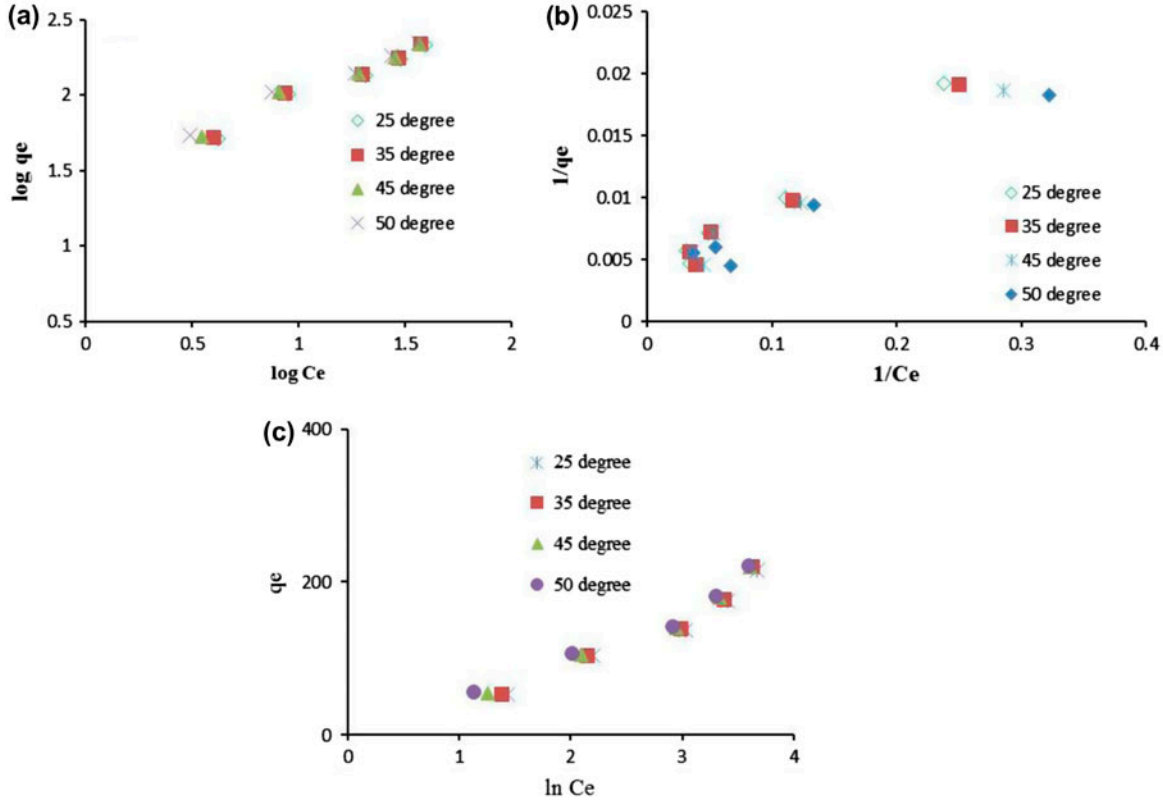

Fig. 5. (a) Langmuir, (b) Freundlich, and (c) Temkin isotherm models for the adsorption of Hg^{2+} metal ion using ARSA.

Table 3
Comparison of maximum monolayer adsorption capacity of Hg^{2+} on various adsorbents

Adsorbents	Maximum monolayer adsorption capacity (mg g^{-1})	Refs.
Silica	196.6	[43]
Multi-walled carbon nanotubes	84.6	[44]
Magnetic mesoporous silica composites	19.79	[45]
Polystyrene-coated $CoFe_2O_4$ particles	86.9	[46]
Silica-coated Fe_3O_4 nanoparticle	148.8	[47]
Thiol-derivatized single-walled carbon nanotube	151.5	[48]
Sulfur incorporated MWCNT	113.64	[49]
Polyrhodanine-encapsulated magnetic nanoparticles	179	[50]
ARSA	270.2	Present study

Table 4
Thermodynamics parameters for the adsorption of Hg^{2+} onto ARSA (Hg^{2+} concentration 100 mg L^{-1}; temperature range 25–45°C)

			ΔG° (J mol^{-1})			
Q_m (mg L^{-1})	ΔH° (kJ mol^{-1})	ΔS° (J mol^{-1} K^{-1})	298 K	308 K	313 K	318 K
100	79.87	0.26	−0.59	−3.29	−4.64	−5.99

better correlation coefficient values ($R^2 > 0.98$) than other two studied isotherm models which designated the superior applicability of this model.

A comparison of maximum monolayer adsorption capacity of Hg^{2+} onto various adsorbents is shown in Table 3 [43–50]. The maximum monolayer adsorption capacity of ARSA was higher than most adsorbents shown in Table 3.

3.2. Thermodynamic studies

The adsorption of Hg^{2+} was studied at different temperatures from 25 to 50°C at pH 6 for 90 min (Fig. 2(b)). The adsorption of Hg^{2+} was increased from 42.3 to 85.6% as the temperature increased from 25 to 50°C, which showed the endothermic nature of Hg^{2+} adsorption onto ARSA. The dependence of temperature on the adsorption process is connected with several thermodynamic parameters viz. ΔG°, ΔH°, and ΔS°. The values of ΔH° and ΔS° were found from the slopes and intercepts of the plots of $\ln K_c$ vs. $1/T$ using this equation:

$$\ln K_c = -\frac{\Delta H^\circ}{RT} + \frac{\Delta S^\circ}{R} \quad (8)$$

The values of thermodynamic parameters for Hg^{2+} adsorption onto ARSA are given in Table 4. The values of ΔH° were positive (79.87 kJ mol^{-1}), which indicated that the adsorption of Hg^{2+} onto ARSA was endothermic in nature. The positive values ΔS° (0.26 J mol^{-1} K^{-1}) indicated an increase in the randomness. The negative values of ΔG° showed the degree of spontaneity of the adsorption process.

4. Conclusions

In the present study, alizarin red-S-loaded amberlite IRA-400 resin was used for the adsorption of one of the most toxic Hg^{2+} metal ion from aqueous medium. In the beginning, the rate of adsorption of Hg^{2+} onto ARSA was rapid, followed by decreasing rates, until an almost constant value. It was also noted that the adsorption was immensely dependent upon various parameters. The maximum adsorption of Hg^{2+} onto ARSA was noted at pH 6 and 45°C. The adsorption of Hg^{2+} onto ARSA followed pseudo-second-order kinetics and the equilibrium data fitted well with Freundlich isotherm. The maximum monolayer adsorption capacity (q_m) was 303.03 mg g^{-1} at 25°C. Moreover, the results of thermodynamic study showed that Hg^{2+} adsorption onto ARSA was endothermic and spontaneous. The more negative values of free energy with the increase in temperatures indicated that the Hg^{2+} adsorption onto ARSA was favored at high temperatures. The negative value of entropy change showed that orderliness of the adsorbed system was higher than the pre-adsorption solution phase. The four adsorption–desorption cycles revealed that ARSA was suitable for reuse in the

removal of Hg^{2+} metal ion, effectively. Subsequently, ARSA had wide applicability and encouraging in the removal of heavy metal ions from polluted waters.

Acknowledgment

The authors would like to extend their sincere appreciation to the Deanship of Scientific Research at King Saud University for funding this work through the Research Group no. RG-1436-034.

References

[1] M.E. Mahmoud, O.F. Hafez, A. Alrefaay, M.M. Osman, Performance evaluation of hybrid inorganic/organic adsorbents in removal and preconcentration of heavy metals from drinking and industrial waste water, Desalination 253 (2010) 9–15.
[2] S.M. Alshehri, M. Naushad, T. Ahamad, Z.A. Alothman, A. Aldalbahi, Synthesis, characterization of curcumin based ecofriendly antimicrobial bio-adsorbent for the removal of phenol from aqueous medium, Chem. Eng. J. 254 (2014) 181–189.
[3] Mu. Naushad, Z.A. Alothman, Separation of toxic Pb2+ metal from aqueous solution using strongly acidic cation-exchange resin: analytical applications for the removal of metal ions from pharmaceutical formulation, Desalin. Water Treat., 53 (2015) 2158–2166.
[4] M. Naushad, Z.A. ALOthman, M.R. Khan, N.J. ALQahtani, I.H. ALSohaimi, Equilibrium, kinetics and thermodynamic studies for the removal of organophosphorus pesticide using Amberlyst-15 resin: Quantitative analysis by liquid chromatography–mass spectrometry, J. Ind. Eng. Chem. 20 (2014) 4393–4400.
[5] F. Fu, Q. Wang, Removal of heavy metal ions from wastewaters: A review, J. Environ. Manage. 92 (2011) 407–418.
[6] M.R. Awual, M.M. Hasan, A. Shahat, M. Naushad, H. Shiwaku, T. Yaita, Investigation of ligand immobilized nano-composite adsorbent for efficient cerium (III) detection and recovery, Chem. Eng. J. 265 (2015) 210–218.
[7] M.R. Awual, T. Yaita, H. Shiwaku, S. Suzuki, A sensitive ligand embedded nano-conjugate adsorbent for effective cobalt(II) ions capturing from contaminated water, Chem. Eng. J. 276 (2015) 1–10.
[8] G. Sharma, D. Pathania, M. Naushad, Fabrication, characterization and antimicrobial activity of polyaniline Th(IV) tungstomolybdophosphate nanocomposite material: Efficient removal of toxic metal ions from water, Chem. Eng. J. 251 (2014) 413–421.
[9] G. Sharma, D. Pathania, M. Naushad, Preparation, characterization and antimicrobial activity of biopolymer based nanocomposite ion exchanger pectin zirconium(IV) selenotungstophosphate: Application for removal of toxic metals, J. Ind. Eng. Chem. 20 (2014) 4482–4490.
[10] A. Sigel, H. Sigel, Metal Ions in Biological Systems, Mercury and its Effects on Environment and Biology, vol. 34, Dekker, New York, NY, 1997.
[11] T.W. Clarkson, Mercury: Major issues in environmental health, Environ. Health Perspect. 100 (1992) 31–38.
[12] L. Wang, R. Xing, S. Liu, S. Cai, H. Yu, J. Feng, R. Li, P. Li, Synthesis and evaluation of a thiourea-modified chitosan derivative applied for adsorption of Hg(II) from synthetic wastewater, Int. J. Biol. Macromol. 46 (2010) 524–528.
[13] C. Sun, R. Qu, C. Ji, Q. Wang, C. Wang, Y. Sun, G. Cheng, A chelating resin containing S, N and O atoms: Synthesis and adsorption properties for Hg(II), Eur. Polym. J. 42 (2006) 188–194.
[14] S.A. Nabi, M. Naushad, A new electron exchange material Ti(IV) iodovanadate: Synthesis, characterization and analytical applications, Chem. Eng. J. 158 (2010) 100–107.
[15] P. Miretzky, A.F. Cirelli, Hg(II) removal from water by chitosan and chitosan derivatives: A review, J. Hazard. Mater. 167 (2009) 10–23.
[16] M.F. Yardim, T. Budinova, E. Ekinci, N. Petrov, M. Razvigorova, V. Minkova, Removal of mercury(II) from aqueous solution by activated carbon obtained from furfural, Chemosphere 52 (2003) 835–841.
[17] M. Zabihi, A. Ahmadpour, A. Asl, Removal of mercury from water by carbonaceous sorbents derived from walnut shell, J. Hazard. Mater. 167 (2009) 230–236.
[18] E.I. Unuabonah, K.O. Adebowale, B.I. Olu-Owolabi, Kinetic and thermodynamic studies of the adsorption of lead(II) ions onto phosphate-modified kaolinite clay, J. Hazard. Mater. 144 (2007) 386–395.
[19] A.B. Pérez-Marín, V.M. Zapata, J.F. Ortuño, M. Aguilar, J. Sáez, M. Lloréns, Removal of cadmium from aqueous solutions by adsorption onto orange waste, J. Hazard. Mater. 139 (2007) 122–131.
[20] A. Kumar, G. Sharma, M. Naushad, P. Singh, S. Kalia, Polyacrylamide/$Ni_{0.02}Zn_{0.98}O$ nanocomposite with high solar light photocatalytic activity and efficient adsorption capacity for toxic dye removal, Ind. Eng. Chem. Res. 53 (2014) 15549–15560.
[21] M. Arias, M.T. Barral, J. Da Silva-Carvalhal, J.C. Mejuto, D. Rubinos, Interaction of Hg(II) with kaolin-humic acid complexes, Clay Miner. 39 (2004) 35–45.
[22] S.A. Nabi, M. Naushad, A.M. Khan, Sorption studies of metal ions on napthol blue–black modified Amberlite IR-400 anion exchange resin: Separation and determination of metal ion contents of pharmaceutical preparation, Colloids Surf., A 280 (2006) 66–70.
[23] J.U.K. Oubagaranadin, N. Sathyamurthy, Z.V.P. Murthy, Evaluation of Fuller's earth for the adsorption of mercury from aqueous solutions: A comparative study with activated carbon, J. Hazard. Mater. 142 (2007) 165–174.
[24] D. Pathania, G. Sharma, M. Naushad, V. Priya, A biopolymer-based hybrid cation exchanger pectin cerium(IV) iodate: Synthesis, characterization, and analytical applications, Desalin. Water Treat., Article in press, (2015), doi:10.1080/19443994.2014.967731.
[25] S.A. Nabi, M. Naushad, A.M. Khan, Sorption studies of metal ions on napthol blue–black modified Amberlite IR-400 anion exchange resin: Separation and determination of metal ion contents of pharmaceutical preparation, Colloids Surf., A 280 (2006) 66–70.

[26] A. Lezzi, S. Cobianco, Chelating resins supporting dithiocarbamate and methylthiourea groups in adsorption of heavy metal ions, J. Appl. Polym. Sci. 54 (1994) 889–897.
[27] S. Pramanik, P.K. Dhara, P. Chattopadhyay, A chelating resin containing bis(2-benzimidazolylmethyl) amine: Synthesis and metal-ion uptake properties suitable for analytical application, Talanta 63 (2004) 485–490.
[28] R.J. Qu, C.H. Wang, C.M. Sun, C.N. Ji, G.X. Cheng, X.Q. Wang, G. Xu, Syntheses and adsorption properties for Hg^{2+} of chelating resin of crosslinked polystyrene-supported 2,5-dimercapto-1,3,4-thiodiazole, J. Appl. Polym. Sci. 92 (2004) 1646–1652.
[29] J.M. Sánchez, M. Hidalgo, V. Salvadó, The selective adsorption of gold(III) and palladium(II) on new phosphine sulphide-type chelating polymers bearing different spacer arms, React. Funct. Polym. 46 (2001) 283–291.
[30] S.A. Nabi, M.A. Khan, A. Islam, Adsorption of metal ions on modified anion-exchange resin selective separation of Fe^{3+} and Hg^{2+} from other metals, Acta Chromatogr. 11 (2001) 130–138.
[31] Z.A. AL-Othman, Inamuddin, M. Naushad, Forward (M^{2+}−H^{+}) and reverse (H^{+}−M^{2+}) ion exchange kinetics of the heavy metals on polyaniline Ce(IV) molybdate: A simple practical approach for the determination of regeneration and separation capability of ion exchanger, Chem. Eng. J. 171 (2011) 456–463.
[32] M.M. Alam, Z.A. ALOthman, Mu. Naushad, Analytical and environmental applications of polyaniline Sn (IV) tungstoarsenate and polypyrrole polyantimonic acid composite cation-exchangers, J. Ind. Eng. Chem. 19 (2013) 1973–1980.
[33] S.A. Nabi, A.M. Khan, Synthesis, ion exchange properties and analytical applications of stannic silicomolybdate: Effect of temperature on distribution coefficients of metal ions, React. Funct. Polym. 66 (2006) 495–508.
[34] J. Lehto, R. Harjula, H. Leinonen, A. Paajanen, T. Laurila, K. Mononen, L. Saarinen, Advanced separation of harmful metals from industrial waste effluents by ion exchange, J. Radioanal. Nucl. Chem. Art. 208 (1996) 435–443.
[35] M. Naushad, Surfactant assisted nano-composite cation exchanger: Development, characterization and applications for the removal of toxic Pb^{2+} from aqueous medium, Chem. Eng. J. 235 (2014) 100–108.
[36] M. Naushad, Z.A. ALOthman, G. Sharma, Inamuddin, Kinetics, isotherm and thermodynamic investigations for the adsorption of Co(II) ion onto crystal violet modified amberlite IR-120 resin, Ionics 21 (2015) 1453–1459.
[37] N. Azouaou, M. Belmedani, H. Mokaddem, Z. Sadaoui, Adsorption of lead from aqueous SOLUTION onto untreated orange barks, Chem. Eng. Trans. 32 (2013) 55–60.
[38] S. Lagergren, About the theory of so called adsorption of soluble substances, KungligaSvenskaVetenskapsakademiens, Handlingar, Band 24 (1898) 1–39.
[39] Y.S. Ho, G. McKay, D.A.J. Wase, C.F. Forster, Study of the sorption of divalent metal ions on to peat, Adsorpt. Sci. Technol. 18 (2000) 639–650.
[40] I. Langmuir, The constitution and fundamental properties of solids and liquids. Part I. Solids, J. Am. Chem. Soc. 38 (1916) 2221–2295.
[41] H.M.F. Freundlich, Over the adsorption in solution, J. Phys. Chem. 57 (1906) 385–470.
[42] M.I. Temkin, V. Pyzhev, Kinetics of ammonia synthesis on promoted iron catalyst, Acta Physiochim. URSS 12 (1940) 327–356.
[43] L.N.H. Arakaki, V.S. Filha, K.S. de Sousa, F.P. Aguiar, M.G. da Fonseca, J.G.P. Espinola, Silica gel ethyleneimine and its adsorption capacity for divalent Pb, Cd, and Hg, Thermochim. Acta 440 (2006) 176–180.
[44] M. Hadavifar, N. Bahramifar, H. Younesi, Q. Li, Adsorption of mercury ions from synthetic and real wastewater aqueous solution by functionalized multi-walled carbon nanotube with both amino and thiolated groups, Chem. Eng. J. 237 (2014) 217–228.
[45] B.Y. Song, Y. Eom, T.G. Lee, Removal and recovery of mercury from aqueous solution using magnetic silica nanocomposites, Appl. Surf. Sci. 257 (2011) 4754–4759.
[46] K. Jainae, N. Sukpirom, S. Fuangswasdi, F. Unob, Adsorption of Hg(II) from aqueous solutions by thiol-functionalized polymer-coated magnetic particles, J. Ind. Eng. Chem. 23 (2015) 273–278.
[47] P.I. Girginova, A.L. Daniel-da-Silva, C.B. Lopes, P. Figueira, M. Otero, V.S. Amaral, E. Pereira, T. Trindade, Silica coated magnetite particles for magnetic removal of Hg^{2+} from water, J. Colloid Interface Sci. 345 (2010) 234–240.
[48] N.M. Bandaru, N. Reta, H. Dalal, A.V. Ellis, J. Shapter, N.H. Voelcker, Enhanced adsorption of mercury ions on thiol derivatized single wall carbon nanotubes, J. Hazard. Mater. 261 (2013) 534–541.
[49] A. Gupta, S.R. Vidyarthi, N. Sankararamakrishnan, Enhanced sorption of mercury from compact fluorescent bulbs and contaminated water streams using functionalized multiwalled carbon nanotubes, J. Hazard. Mater. 274 (2014) 132–144.
[50] J. Song, H. Kong, J. Jang, Adsorption of heavy metal ions from aqueous solution by polyrhodanine-encapsulated magnetic nanoparticles, J. Colloid Interface Sci. 359 (2011) 505–511.